How to cite: *Angew. Chem. Int. Ed.* **2024**, *63*, e202401004
doi.org/10.1002/anie.202401004

CRISPR/Cas9

Near-Infrared Light Activated Formulation for the Spatially Controlled Release of CRISPR-Cas9 Ribonucleoprotein for Brain Gene Editing

Susana Simões, Miguel Lino, Angela Barrera, Catarina Rebelo, Francesca Tomatis, Andreia Vilaça, Christopher Breunig, Andrea Neuner, João Peça, Ricardo González, Alexandra Carvalho, Stefan Stricker, and Lino Ferreira**

Abstract: The CRISPR/Cas9 system has emerged as a promising platform for gene editing; however, the lack of an efficient and safe delivery system to introduce it into cells continues to hinder clinical translation. Here, we report a rationally designed gene-editing nanoparticle (NP) formulation for brain applications: an sgRNA:Cas9 ribonucleoprotein complex is immobilized on the NP surface by oligonucleotides that are complementary to the sgRNA. Irradiation of the formulation with a near-infrared (NIR) laser generates heat in the NP, leading to the release of the ribonucleoprotein complex. The gene-editing potential of the formulation was demonstrated *in vitro* at the single-cell level. The safety and gene editing of the formulation were also demonstrated in the brains of reporter mice, specifically in the subventricular zone after intracerebral administration and in the olfactory bulb after intranasal administration. The formulation presented here offers a new strategy for the spatially controlled delivery of the CRISPR system to the brain.

[*] S. Simões, M. Lino, A. Barrera, C. Rebelo, F. Tomatis, A. Vilaça, J. Peça, R. González, A. Carvalho, L. Ferreira
CNC-Centre for Neuroscience and Cell Biology of University of Coimbra, Portugal
E-mail: susana.simoes@cnc.uc.pt
lino.ferreira@uc.pt

S. Simões, C. Rebelo, F. Tomatis, A. Vilaça, R. González, A. Carvalho
Institute of Interdisciplinary Research of University of Coimbra, Portugal

M. Lino, A. Barrera, L. Ferreira
Faculty of Medicine, University of Coimbra, Coimbra, Portugal

C. Breunig, A. Neuner, S. Stricker
Epigenetic Engineering, Institute of Stem Cell Research, Helmholtz Zentrum, Germany

J. Peça
Department of Life Science, University of Coimbra, Coimbra, Portugal

Genome editing using clustered regularly interspaced short palindromic repeats (CRISPR)/CRISPR-associated protein 9 (Cas9)[1] has high potential for the treatment of neurological diseases originating from genetic mutations, including Alzheimer disease,[2] Huntington disease,[3] and amyotrophic lateral sclerosis,[4] among others. Many of the advances made in CRISPR brain delivery systems have been achieved by taking advantage of viral vectors, specifically adeno-associated viruses (AAVs). However, AAVs have a low packing capacity, require specific infrastructure for large-scale production, and pose safety concerns due to their immunogenicity[5] and ability to integrate into the DNA breaks created by Cas9.[6] Nonviral CRISPR/Cas delivery systems have emerged as alternatives to viral delivery approaches. Nonviral formulations have been used in the context of the adult brain[7] to deliver different cargos, including plasmid DNA encoding Cas9 and sgRNA,[8] Cas9 mRNA plus sgRNA[9] and Cas9 ribonucleoprotein (Cas9 complexed with sgRNA),[7c] among which the last two are the most desirable for clinical translation. These nonviral vectors, administered intracerebrally, have allowed successful gene editing in different types of brain cells.[7a,b,e,10] One of the limitations of existing nonviral vectors is their limited spatial resolution. Once injected, nanoparticles (NPs) can diffuse from the injection site into the brain parenchyma depending on their morphology and chemistry.[11] The spatial control of gene editing requires light-activatable NPs,[12] particularly near-infrared (NIR) light-activatable NPs, since NIR has deeper tissue penetration (millimeter range[13]). NIR-activatable CRISPR formulations have been reported for use in gene editing outside the brain (Figure S1), in certain tumor models,[8a,14] through the use of Cas9/sgRNA-encoding plasmids[8,15] and the Cas9/sgRNA ribonucleoprotein complex (RNP),[14,16] but not inside the brain. These formulations have important limitations, such as (i) limited gene editing efficiency (<10% of the cells);[8b] (ii) high laser power requirements for releasing the gene editing system, which can compromise cell viability;[14b] (iii) leaching of the formulation in the absence of NIR activation;[15,17] and (iv) lanthanide components that may induce toxicity.[16] In addition, the application of NIR-activatable CRISPR formulations in the brain presents significant challenges because (i) the laser should penetrate

the skull to activate brain cells transfected with the NPs; (ii) the triggering system should not activate gliosis; and (iii) the NP activation should display spatial resolution.

Here, we report an NIR light-triggerable NP formulation for gene editing in the brain with improved spatial control. The Cas9 protein rather than Cas9 DNA was selected for delivery to prevent immunogenic responses.[18] In this formulation, complementary oligonucleotides (ssDNA) immobilized on gold nanorods (AuNRs) are used to immobilize the complex sgRNA:Cas9 (RNP). The AuNRs can absorb near-infrared (NIR) light and convert it into heat, which induces dehybridization of the complementary sgRNA from immobilized ssDNA immobilized on the surface of the AuNRs (Figure 1a). The oligo spacer and composition of the formulation were rationally designed to (i) minimize leaching of the ribonucleoprotein complex in the absence of laser activation, (ii) prevent cleavage by the Cas9 system (Figure 1b) and (iii) prevent denaturation of the Cas9 protein. The gene editing properties of this formulation were evaluated *in vitro* using brain cells and *in vivo* following intracerebral or intranasal administration in a reporter transgenic mouse.

To immobilize the RNP on the AuNR core, we selected an ssDNA sequence of 20 bases complementary to the sgRNA that was modified at the 3' or 5' terminus with different poly(thymine) spacers (8, 16 and 32) and contained a terminal thiol group to allow covalent attachment to the AuNR surface (Figure 1b and S3a). The poly(thymine) spacer was used to distance the oligonucleotide hybridization sequence from the AuNR surface. The length of the spacers was selected on the basis of molecular modeling studies (see below). As a control, we used a sequence of 20 bases without complementarity to the sgRNA (NC). The average length and width of the AuNRs were 42 ± 0.3 nm and 13 ± 0.2 nm, respectively (Figure S2). The average number of ssDNA molecules per AuNR was 403 ± 28, with a coupling efficiency of nearly 40 % (Figure S3c). Next, we evaluated whether the ssDNA molecules immobilized on the surface of the AuNRs were accessible for hybridization with sgRNA. With the exception of the noncomplementary (NC) ssDNA, the sgRNA was able to hybridize with all the other AuNR-ssDNA formulations (Figure S3b). Thus, the interaction between the sgRNA and the AuNRs seems to be mediated by nucleotide complementarity and not by other interactions. To evaluate the release properties of the formulation, the AuNR-ssDNA was hybridized with the sgRNA and then irradiated by an NIR laser. The activation of AuNR-dsDNA:sgRNA by an NIR laser at a power of 1000 mW increased the temperature of the suspension from 21 °C to 41 °C (Figure S3d), leading to the release of approximately 60 % of the immobilized sgRNA from the formulation in 10 min (Figure S3e). Next, the AuNR-ssDNA formulations were exposed to the RNP for 1 h at room temperature to allow hybridization of the RNP to the complementary ssDNA immobilized on the AuNR. The immobilization efficiency was slightly greater (more than 60 %) for the formulations containing ssDNA with 16 or 32 thymines than for the formulation containing ssDNA with 8 thymines (Figure S4a). The immobilization of the RNPs on the AuNR-ssDNA altered the zeta potential from −40 mV to −20 mV (Figure S4b). The formulations resulting from the hybridization of the RNPs with the immobilized oligonucleotides, AuNR-dsDNA*n*T-RNP, were relatively stable for 24 h in water, as no significant changes were observed in the absorbance spectrum (Figure S4c). Importantly, the Cas9 enzyme was not able to cleave the double-stranded DNA that resulted from hybridization between the *target* sequence of the sgRNA and the ssDNA (Figure S4d).

We performed molecular dynamics (MD) analyses to investigate the interaction of the sgRNA with the ssDNA. Because the ssDNA is covalently attached to the AuNRs, the interaction between the 20-base complementary ssDNA and the sgRNA is dependent on the length of the poly-(thymine) spacer. The spacer needs to be long enough for the 20 nt complementary ssDNA to reach the sgRNA strand in the enzyme pocket.[19] Moreover, both the ssDNA and spacer length should be rationally designed to prevent the cleavage of the ssDNA by *sp*Cas9, since the enzyme may cleave ssDNA even in the absence of a protospacer adjacent motif (PAM sequence).[20] The width of the enzyme from one side to the other is approximately 80 Å, assuming that the interphosphate distance of ssDNA can range between 5.9 Å and 7 Å depending on the sugar pucker,[2,21] and an 8T spacer extends only 52 Å, which is roughly half of the protein width; thus, with an 8T spacer, only a few bases can reach the complementary sgRNA (Figure 1c-i). For the longer spacers (16T and 32T), we modeled possible hybridization levels between the ssDNA and sgRNA. According to the simulations for the complex with ssDNA-16T, if 6 bases of the spacer remained outside the protein, only 14 out of the 20 bases could reach the sgRNA for hybridization (Figure 1c-ii). With the longer spacer (ssDNA-32T), 24 bases of the spacer were accessible to the solvent when 14 bases of the ssDNA were hybridized. We also modeled the fully hybridized complex with ssDNA-32T (Figure 1c-iii), in which 11 bases were accessible to the solvent. The MD simulations showed that the protein equilibration was relatively rapid (Figure S5). Overall, the 8T spacer is not long enough for the immobilization of the RNP on the AuNR; however, both the 16T and 32T spacers allow the ssDNA to hybridize with the sgRNA in the enzyme pocket.

Next, the release of the RNP from the AuNR formulation after NIR irradiation was evaluated. First, we evaluated the thermostability of the Cas9 enzyme after NIR activation (Figure S6). Cas9 protein has been shown to lose its stability at temperatures above 45 °C.[22] The soluble Cas9 enzyme was incubated with AuNRs (without ssDNA conjugation), exposed to an NIR laser at different powers for 3 min (Figure S6b, c) and then centrifuged to collect the supernatant. The protein was quantified, and its enzyme activity was tested. NIR laser powers above 800 mW/cm^2 caused denaturation and subsequent precipitation of the enzyme. However, Cas9 collected from a colloidal suspension of AuNRs activated at 700 mW/cm^2 (or even at 1000 mW/cm^2) and transfected with sgRNA and RNAiMAX into d2eGFP-HeLa cells (Figure S6d, e) exhibited activity. Thus, for the release studies of RNP from AuNRs, we used an NIR laser at 700 mW/cm^2 for 3 min. In these conditions, approximately

a

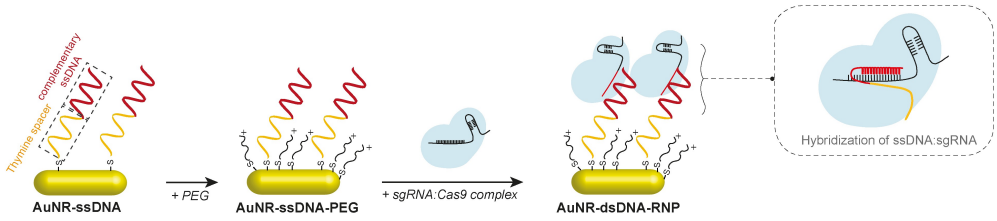

b

Name	ssDNA sequence	Mw (Da)
ssDNA8T(3´)	5'-GACACGCTGAACTTGTGGCCTTTTTTT-C6-HS-3'	8747.8
ssDNA16T(3')	5'-GACACGCTGAACTTGTGGCCTTTTTTTTTTTTTTT-C6-HS-3'	11181.4
ssDNA32T(3')	5´-GACACGCTGAACTTGTGGCCTTTTTTTTTTTTTTTTTTTTTTTTTTTTTTTT-C6-HS-3'	16048.6
ssDNA16T(5')	5´-HS-C6-TTTTTTTTTTTTTTTTGACACGCTGAACTTGTGGCC-3´	11181.4
ssDNA16T(5´, NC)	5'-TGTCCAGATCCAGTGCAGCGTTTTTTTTTTTTTTT-C6-HS-3'	11181.4

c

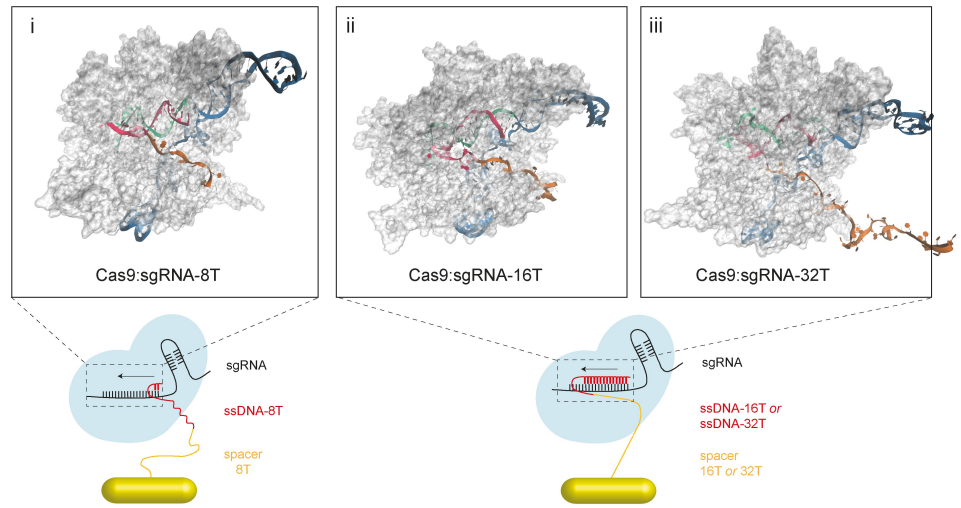

d

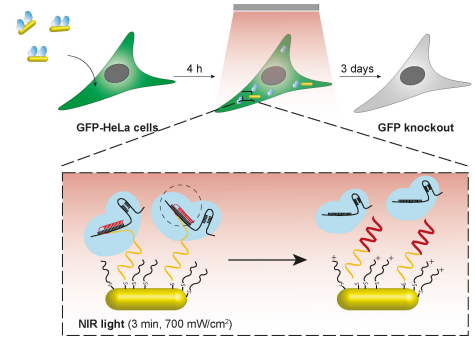

e

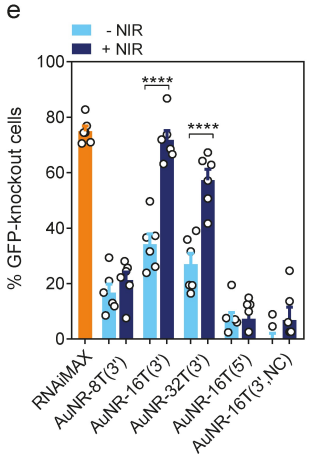

f

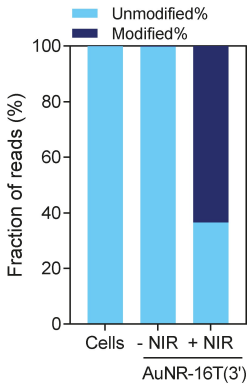

***Figure 1. In vitro* delivery of Cas9-RNP for efficient genome editing**. (a) Schematic representation of the synthesis of the gene editing formulations. (b) Oligonucleotide sequences used for immobilization on the AuNRs. (c) Representative structures of the Cas9 system with different spacer lengths. The representations in the top panel correspond to cluster structures from the simulated systems. In blue, the sgRNA (nonhybridized); in green, the sgRNA bases that are hybridized to the ssDNA (red); and, in orange, the poly(thymine) spacer. (d) Schematic representation of the NIR light-controlled release of RNP for gene editing. The HeLa-d2eGFP cells were incubated with the AuNR-dsDNA-RNP formulations for 4 h and then washed. Fresh medium was added, and the cells were irradiated for 3 min with an NIR laser. After 72 h, eGFP knockout was monitored via a high-content fluorescence microscope. (e) Percentage of GFP-knockout cells. RNAiMAX lipofectamine was used as a positive control. The eGFP fluorescence was normalized to the nontreated cells. The data are expressed as the mean ± SEM ($n = 2–6$). One-way ANOVA with Tukey's post hoc multiple comparisons test was performed: (****), $p < 0.0001$. (f) Allele frequency in HeLa cells edited with the AuNR-dsDNA(16T)-RNP formulation.

31.5 % of the RNP was released from the formulation (Figure S4e).

To evaluate the cellular uptake of AuNR-dsDNA-RNP, HeLa cells were transfected with each formulation containing different spacers (8T, 16T and 32T) (50 μg/mL) for 4 h, after which the concentration of gold within the cells was measured via inductive coupled plasma mass spectrometry (ICP-MS) (Figure S7a). Our results showed different levels of cellular uptake of the different formulations, and the AuNR-dsDNA(16T)-RNP formulation had the highest internalization, likely facilitated by its aggregation and subsequent sedimentation in cell culture medium (Figure S7b). To evaluate the intracellular trafficking of the formulations, Cas9 was labeled with DyLight 650 (DL) before the formation of the complex with the sgRNA. The AuNR-dsDNA(16T)-RNP-DL was incubated with HeLa cells and activated with an NIR laser (780 nm, power: 700 mW/cm^2, 3 min). The intracellular trafficking of AuNR-dsDNA-RNP was characterized by confocal microscopy after staining the endolysosomal compartment with LysoTracker Red (Figure S7c). Our results indicate that the exposure of the cells to NIR contributed to endolysosomal escape of the nanocarrier (Figure S7d). TEM analyses revealed that the exposure of cells to NIR increased the number of disrupted endolysosomes (Figure S7e and f). To further determine whether AuNR-dsDNA-RNP disrupted the endolysosomal compartment, we used immunofluorescence to monitor galectin-9, a membrane damage sensor that has been used to observe the endosomal escape of therapeutic molecules.[23] Hydroxychloroquine, which has been shown to induce endolysosomal membrane damage,[23] was used as a positive control. Indeed, the cells exposed to AuNR-dsDNA(32T)-RNP and activated by an NIR laser presented more galectin-9 foci than those without laser activation, suggesting disruption of the endolysosomal compartment (Figure S8). Overall, our results indicated that the degree of cellular internalization of AuNRs-dsDNA-RNP depends on the length of the ssDNA and that escape from the endolysosomal compartment is increased by activation of the formulation by NIR light.

To evaluate the gene editing potential of the formulations, the different AuNR-dsDNA-RNP formulations were used to knockout the eGFP fluorescence in d2eGFP-HeLa cells. For this purpose, cells were transfected with each formulation (50 μg/mL) for 4 h in cell culture medium, either irradiated or not irradiated at 780 nm (700 mW/cm^2) for 3 min and finally cultured for 3 days (Figure 1d). The cell viability and eGFP knockout were evaluated via high-content microscopy. Cells transfected with AuNR-dsDNA16T-RNP decreased in number after light activation, indicating the cytotoxicity of the formulation (Figure S9). The remaining formulations had negligible effects on cell viability. Cells treated with the formulations but without light activation showed low eGFP knockout activity, below 30 % in the AuNR-dsDNA32T-RNP formulation (Figure 1e). Importantly, cells transfected with AuNR-dsDNA16T-RNP or AuNR-dsDNA32T-RNP and activated by light showed eGFP knockout comparable to that observed in cells transfected with Lipofectamine RNAiMAX complexed with RNP, which was used as a positive control (Figure 1e). Gene editing was further confirmed by Illumina NGS analyses, and indels (~64 %) were observed around the intended cleavage site (Figure 1f and S10), further confirming the occurrence of cellular gene editing. As expected, the edited cells showed low eGFP expression for several passages, demonstrating a biological effect over time (Figure S11a). Gene editing can be initiated by NIR laser activation immediately after cell transfection (4 h after exposure to the formulation) or 20 h after cell transfection; thus, the timing of the biological process can be controlled (Figure S11b). Furthermore, the AuNR formulation enabled gene editing with single-cell resolution when confocal microscopy was used for NIR activation (Figure S11c). Importantly, AuNRs bound to an ssDNA sequence complementary to the sgRNA were critical for the immobilization of the RNP on the AuNR-ssDNA system. Formulations containing ssDNA that was not complementary to the terminal sequence of the sgRNA or that was inverted (the thymines were included at the 5' rather than the 3' end) were not active (Figure S12). Overall, our results demonstrated the capacity of our system to perform gene editing within cells with spatiotemporal control at single-cell resolution. Considering the cell viability and gene editing results, we selected the formulation AuNR-dsDNA32T-RNP for further analyses.

To demonstrate the gene editing of brain cells *in vitro*, subventricular zone (SVZ) cells, astrocytes- and neurons-enriched cells were isolated from Rosa26-tdTomato transgenic Ai9 mice. This mouse has a cassette inserted into the Gt(ROSA)26Sor locus with a LoxP-Stop-LoxP-tdTomato sequence. Two sgRNA sequences ($sgRNA_{loxP1}$ and $sgRNA_{loxP2}$) were designed to enable the deletion of the LoxP-Stop cassette and expression of the tdTomato fluorescent protein (Figure 2a). AuNRs with RNP_{loxP1} and AuNRs with RNP_{loxP2} were prepared separately to allow maximal control of the composition of each formulation. The SVZ cells, astrocytes and neurons were incubated with AuNR-dsDNA(32T)-RNP (equal amounts of AuNR-RNP_{loxP1} and AuNR-RNP_{loxP2}) for 4 h, irradiated or not irradiated with an NIR laser, and then cultured for 1 day (cytotoxicity assay) or 3 days (gene editing assay; Figure 2a). The transfection of brain cells with AuNR-dsDNA(32T)-RNP showed no significant cytotoxicity 24 h after irradiation (Figure S13). In the case of SVZ cells, irradiation was performed after 24 h of incubation with AuNRs because after only 4 h of incubation, most of the formulation was adsorbed in the cell membrane and not internalized (data not shown). The gene editing efficiency was determined by the quantification of tdTomato-positive cells on day 3 post-transfection via flow cytometry. The percentages of tdTomato-expressing SVZ cells, astrocytes and neurons were 8 %, 30 % and 10 %, respectively (Figure 2b–2g). The gene editing efficiency was higher in astrocytes than in SVZ cells, likely because astrocytes internalized a greater concentration of AuNR-dsDNA(32T)-RNP than SVZ cells (Figure S14). Among the SVZ cells, most of the edited cells were immature (Nestin$^+$) (Figure S15a.1 and a.2). However, the highest percentage of gene editing occurred in astrocytes

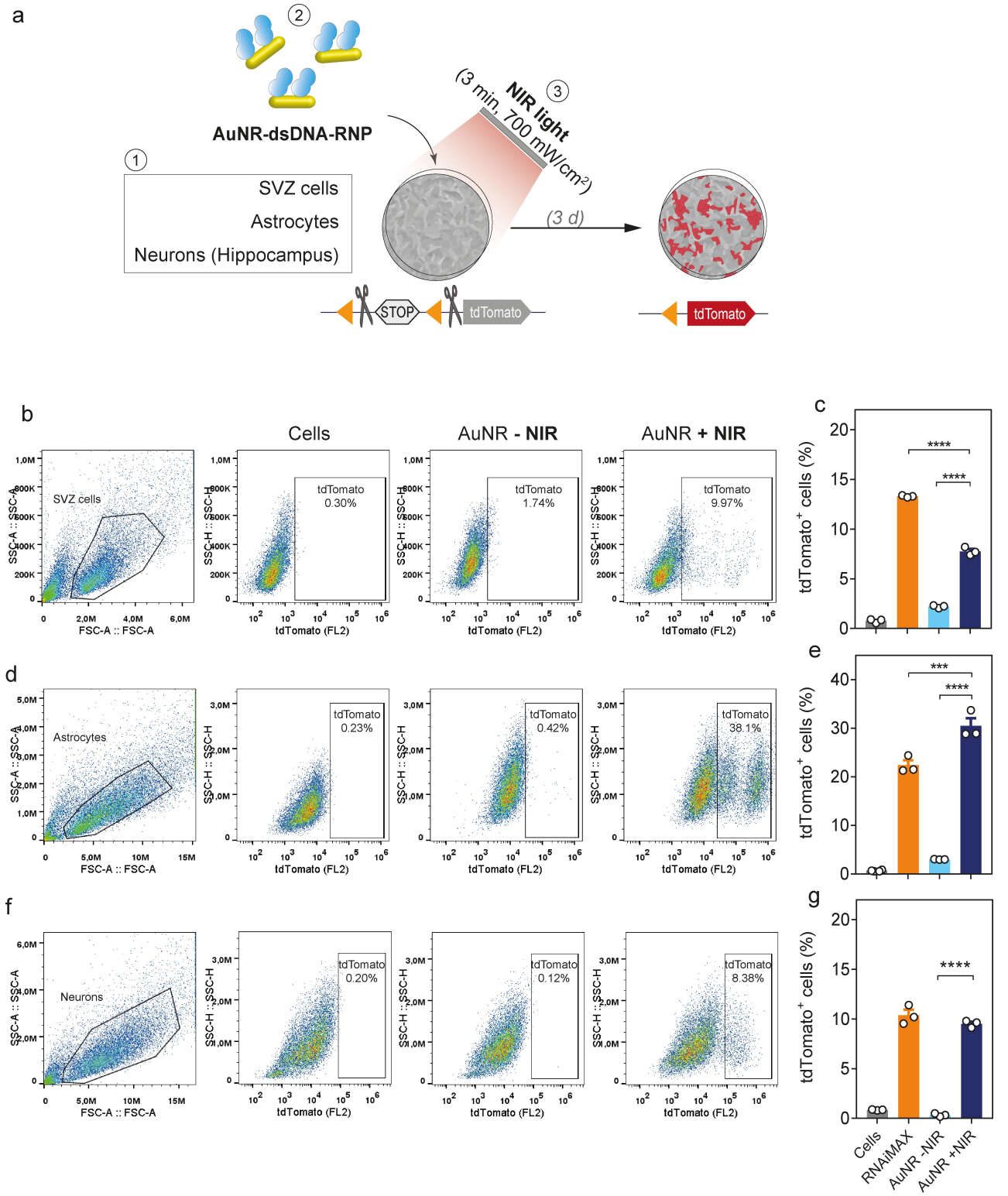

Figure 2. **Gene editing in mouse brain cells by light-activatable AuNR-dsDNA-RNP**. (a) Schematic representation of gene editing in brain cells. The excision of a stop codon by two designed sgRNA sequences leads to the production of the tdTomato fluorescence reporter protein. The cells were transfected with AuNR-dsDNA(32T)-RNP for 4 h, washed, provided with fresh medium and then irradiated for 3 min by an NIR laser at a power of 700 mW/cm^2. After 72 h, tdTomato fluorescence was measured via flow cytometry. (b–f) Representative flow cytometry scatter plots of the SVZ (b), astrocyte- (d) and neurons-enriched populations (f) treated with AuNR-dsDNA32T-RNP with and without NIR light. (c–g) Percentage of tdTomato-positive cells in the SVZ (c), astrocyte- (e) and neuron-enriched populations (g) as assessed by flow cytometry. Positive cells were gated on the basis of the basal expression of tdTomato fluorescence in nontreated cells. In (c), (e) and (g), the results are presented as the mean ± SEM ($n = 3$ independent experiments; 2 replicates per independent experiment). *** and **** denote statistical significance ($p < 0.001$; $p < 0.0001$) assessed by one-way ANOVA followed by Tukey's post hoc test.

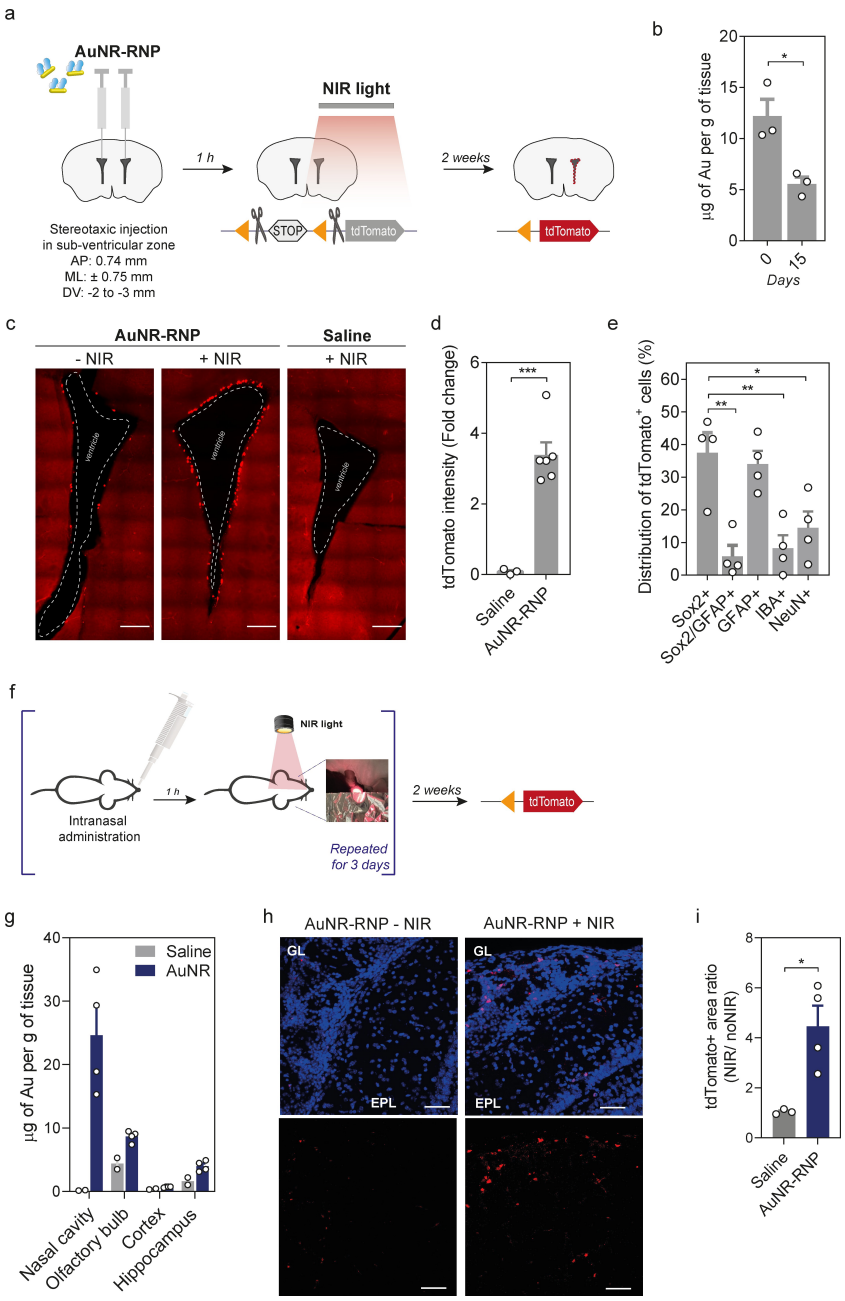

***Figure 3. In vivo* expression of tdTomato in adult Ai9 mice triggered by light-activatable AuNR-dsDNA(32T)-RNP**. (a) Schematic representation of stereotaxic injection of AuNR-dsDNA(32T)-RNP into adult Ai9 mice. (b) AuNR accumulation in the brains of mice after intracerebral administration. Quantification was performed by ICP-MS at 0 and 15 days after the injection. The results are presented as the mean ± SEM ($n = 3$ animals). An unpaired two-sample t test was performed: (*), $p < 0.05$. (c) Representative fluorescence images of tdTomato-positive cells in the irradiated and nonirradiated brain ventricles that received AuNR or saline injection and NIR irradiation. The scale bar represents 300 µm. (d) Fold change in tdTomato fluorescence after NIR light activation. The results are presented as the mean ± SEM ($n = 3$–6 animals, one section per animal). An unpaired two-sample t test was performed: (***), $p < 0.001$. (e) Distribution of tdTomato-positive cells. The results are presented as the mean ± SEM ($n = 4$–5 animals, 3–6 images per marker). *, ** denote statistical significance ($p < 0.05$; $p < 0.01$) assessed by one-way ANOVA followed by Tukey's post hoc test. (f) Experimental setup for intranasal administration. Adult Ai9 mice were intranasally administered (i) AuNR-dsDNA(32T)-RNP or (ii) PBS for 3 days. Each day, 1 h after intranasal administration, part of the skull was irradiated, while the other part was protected with aluminum foil to prevent laser activation. (g) Quantification of AuNR-dsDNA(32T)-RNP in the brain after a single intranasal administration. The animals were sacrificed 4 h post administration. The amount of gold in the nasal cavity, olfactory bulb (OB), cortex and hippocampus was determined via ICP-MS. The results are expressed as the mean ± SEM ($n = 4$ animals for the AuNR group and 2 animals for the saline group) of the % ID (initial dose of Au) per gram of tissue. (h) Representative image of tdTomato expression in irradiated and nonirradiated OBs two weeks after multiple nasal injections. Scale bars = 50 µm. GL: glomerular layer, EPL: external plexiform layer. (i) Quantification of tdTomato fluorescence. The NIR-exposed (+NIR) side was normalized to the nonexposed side of the OB (−NIR). The results are expressed as the mean ± SEM ($n = 4$ animals treated with AuNR-dsDNA(32T)-RNP and $n = 3$ with PBS; 20 to 24 images were obtained from each animal). Statistical analysis was performed by a two-tailed unpaired t test, and * denotes statistical significance ($P = 0.0176$).

(GFAP$^+$ cells) and neurons (NeuN$^+$ cells) (Figure S15b.1–S15c.2). The gene editing in the SVZ cells was further confirmed by Illumina NGS analyses, and indels (~6.4 %) were observed around the intended cleavage site (Figure S16), confirming the occurrence of cellular gene editing. Taken together, our results showed that this approach to the gene editing of brain cells had similar efficacy to that of the commercial transfection agent RNAiMAX (Figure S17), but our system had higher spatial resolution.

To demonstrate the gene editing properties of the formulation *in vivo*, we first evaluated NIR laser penetration. We determined that a 780 nm laser at 1000 mW/cm^2 power delivered through the brain calvaria bone (thickness: 3 mm) exhibited attenuation of 60 % of the initial power (Figure S18) and remained sufficient to knockout up to 50 % of eGFP expression in d2GFP HeLa cells and 25 % of eGFP expression in astrocytes. To demonstrate the gene editing of brain cells *in vivo*, AuNR-dsDNA(32T)-RNP was stereotaxically injected into the subventricular zone of both brain hemispheres of adult Ai9 mice, and only one of the brain hemispheres was exposed to NIR light (Figure 3a and S19). The expression of tdTomato was evaluated two weeks later by confocal microcopy. During this period, the concentration of AuNRs in the brain decreased from 12 μg of AuNRs per g of brain tissue (i.e., 0.3 mg of AuNRs per kg of animal, which is much lower than the brain toxicity of these nanomaterials[24]) to 5 μg of AuNRs per g of brain tissue, as confirmed by ICP-MS analyses (Figure 3b). In other organs, such as the spleen and liver, the concentration of AuNRs increased on day 5, as confirmed by ICP-MS analyses (Figure S19b). Our results showed higher (~4-fold) tdTomato fluorescence in the irradiated hemisphere than in the nonirradiated hemisphere (Figure 3c, d). tdTomato-positive cells were found in immature/progenitor cells (Sox2$^+$; 38 %), astrocytes (GFAP+; ~40 %), microglia (IBA1$^+$; 10 %) and neuronal progenitor cells (NeuN$^+$; 15 %) (Figures 3e and S20). Importantly, we did not observe measurable microglial activation in the region exposed to the NIR laser that underwent gene editing *in vivo* (Figure S21). In a separate experiment, we investigated the possibility of administering AuNR-RNP by a noninvasive route, specifically, by intranasal administration (Figure 3f–3i). Our results showed that most of the AuNRs accumulated in the nasal cavity, followed by the olfactory bulb (Figure 3g). Importantly, gene editing was observed in the irradiated brain hemisphere, particularly in the olfactory bulb. Here, the tdTomato fluorescence was greater (~4-fold) in the irradiated hemisphere than in the nonirradiated hemisphere (Figure 3h and 3i). In conclusion, we developed a gene-editing formulation for on-demand release into deep tissues with high-resolution spatial control upon exposure to transcranial NIR light. This technology offers new possibilities for safely performing brain gene editing.

Supporting Information

The authors have cited additional references within the Supporting Information.[25–28]

Acknowledgements

L.F. acknowledges the funding of COMPETE2020 and FCT programs [PTDC/NAN-MAT/28060/2017 (acronym: BrainEdition), POCI-01-0145-FEDER-016682], Portugal 2020-COMPETE funding through "Programa Operacional Regional do Centro" CENTRO2020 (CENTRO-01-0145-FEDER-000014 and CENTRO-01-0145-FEDER-028060), EC project RESETageing (Ref:952266) and EIC project REGENERAR (Ref:101129812). S.S. acknowledge the FCT fellowships (SFRH/BPD/105327/2014) and the funding by COMPETE2020 and FCT program (EXPL/BIA-CEL/0989/2021 (acronym: Editing_Vision). A.B. and F.T. to the European Commission for the funding through the Marie Skłodowska-Curie Innovative Training Network "NANOSTEM" (n. 764958) for the fellowship. F.T. acknowledge the FCT fellowships (2021/06297/BD) and the PhD Programme in Experimental Biology from University of Coimbra. A.C. and R.G. acknowledge the funding by FCT and CENTRO2020 under the Portuguese Partnership Agreement 2020 by ERDF (2020.10114.BD, IF/01272/2015, and UIDB/04539/2020), and acknowledge computing resources made available by the National Distributed Computing Infrastructure (INCD) funded by FCT and ERDF (01/SAICT/2016 n°. 022153), and the Advanced Computing Project (CPCA/A2/4568/2020 and CPCA/A1/447491/2021). The authors also thank to Luisa Cortes and Microscopy Imaging Center of Coimbra (MICC) for the single cell experiment in the Zeiss LSM 980 Microscope.

Conflict of Interest

The authors declare no conflict of interest.

Data Availability Statement

The data that support the findings of this study are available from the corresponding author upon reasonable request.

Keywords: NIR light activation · Spatial control · CRISPR/Cas9 · Gene editing · Brain

[1] a) M. Jinek, et al., *Science* **2012**, *337*, 816–821; b) L. Cong, et al., *Science* **2013**, *339*, 819–823; c) P. Mali, et al., *Science* **2013**, *339*, 823–826.
[2] B. Gyorgy, et al., *Mol. Ther. Nucleic Acids* **2018**, *11*, 429–440.
[3] S. Yang, et al., *J. Clin. Invest.* **2017**, *127*, 2719–2724.
[4] T. Gaj, et al., *Sci. Adv.* **2017**, *3*, eaar3952.
[5] F. Mingozzi, et al., *Blood* **2013**, *122*, 23–36.
[6] K. S. Hanlon, et al., *Nat. Commun.* **2019**, *10*, 4439.
[7] a) M. Wang, et al., *Proc. Natl. Acad. Sci. USA* **2016**, *113*, 2868–2873; b) B. T. Staahl, et al., *Nat. Biotechnol.* **2017**, *35*, 431–434; c) B. Lee, et al., *Nature Biomedical Engineering* **2018**, *2*, 497–507; d) M. Zuckermann, et al., *Nat. Commun.* **2015**, *6*, 7391; e) H. Park, et al., *Nat. Neurosci.* **2019**, *22*, 524–528.

[8] a) P. Wang, et al., *Angew. Chem. Int. Ed. Engl.* **2018**, *57*, 1491–1496; b) Y. Lyu, et al., *Angew. Chem. Int. Ed. Engl.* **2019**, *58*, 18197–18201.
[9] S. Abbasi, et al., *J. Controlled Release* **2021**, *332*, 260–268.
[10] M. Zuckermann, et al., *Nat. Commun.* **2015**, *6*.
[11] a) E. A. Nance, et al., *Sci. Transl. Med.* **2012**, *4*, 149ra119; b) E. Nance, et al., *ACS Nano* **2014**, *8*, 10655–10664.
[12] W. Cai, et al., *Angew. Chem. Int. Ed. Engl.* **2021**, *60*, 8596–8606.
[13] A. Abdo, et al., *J. Biomed. Opt.* **2013**, *18*, 075001.
[14] a) S. Deng, et al., *Sci. Adv.* **2020**, *6*, eabb4005; b) C. Chen, et al., *Small* **2021**, *17*, e2101155.
[15] L. Li, et al., *Adv. Mater.* **2019**, *31*, e1901187.
[16] Y. Pan, et al., *Sci. Adv.* **2019**, *5*, eaav7199.
[17] H. Yin, et al., *Adv. Funct. Mater.* **2021**, *2107093*, 12.
[18] P. D. Hsu, et al., *Cell* **2014**, *157*, 1262–1278.
[19] a) K. Clement, et al., *Nat. Biotechnol.* **2019**, *37*, 224–226; b) C. Huai, et al., *Nat. Commun.* **2017**, *8*, 1375.
[20] J. Wereszczynski, et al., *Methods Mol. Biol.* **2012**, *819*, 515–524.
[21] D. R. Roe, et al., *J. Chem. Theory Comput.* **2013**, *9*, 3084–3095.
[22] L. B. Harrington, et al., *Nat. Commun.* **2017**, *8*, 1424.
[23] H. Du Rietz, et al., *Nat. Commun.* **2020**, *11*, 1809.
[24] Y. S. Chen, et al., *Nanotechnology* **2010**, *21*, 485102.
[25] B. Nikoobakht, et al., *Chem. Mater.* **2003**, *15*, 1957–1962.
[26] a) A. Wijaya, et al., *Langmuir* **2008**, *24*, 9966–9969; b) M. M. Lino, et al., *Nanoscale* **2017**, *9*, 18668–18680.
[27] C. T. Breunig, et al., *PLoS One* **2018**, *13*.
[28] a) R. Salomon-Ferrer, et al., *WIREs Comput. Mol. Sci.* **2013**, *3*, 198–210; b) I. Ivani, et al., *Nat. Methods* **2016**, *13*, 55–58; c) M. Zgarbová, et al., *J. Chem. Theory Comput.* **2011**, *7*, 2886–2902; d) J.-P. Ryckaert, et al., *J. Comput. Phys.* **1977**, *23*, 327–341; e) T. Darden, et al., *J. Chem. Phys.* **1993**, *98*, 10089–10092; f) H.-P. K. Martin Ester, Jörg Sander, Xiaowei Xu, in *Proceedings of the Second International Conference on Knowledge Discovery and Data Mining*, AAAI Press, Portland, Oregon, **1996**, pp. 226–231.

Manuscript received: January 15, 2024
Version of record online: March 18, 2024